

# Limits on Interactions between Weakly Interacting Massive Particles and Nucleons Obtained with NaI(Tl) Crystal Detectors

K.W. Kim,<sup>1,\*</sup> G. Adhikari,<sup>2</sup> P. Adhikari,<sup>2</sup> S. Choi,<sup>3</sup> C. Ha,<sup>1</sup> I.S. Hahn,<sup>4</sup> E.J. Jeon,<sup>1</sup> H.W. Joo,<sup>3</sup> W.G. Kang,<sup>1</sup> H.J. Kim,<sup>5</sup> N.Y. Kim,<sup>1</sup> S.K. Kim,<sup>3</sup> Y.D. Kim,<sup>1,2</sup> Y.H. Kim,<sup>1,6</sup> Y.J. Ko,<sup>1</sup> H.S. Lee,<sup>1,†</sup> J.S. Lee,<sup>1</sup> J.Y. Lee,<sup>5</sup> M.H. Lee,<sup>1</sup> D.S. Leonard,<sup>1</sup> S.L. Olsen,<sup>1</sup> B.J. Park,<sup>1,7</sup> H.K. Park,<sup>8</sup> H.S. Park,<sup>6</sup> and K.S. Park<sup>1</sup>

(KIMS Collaboration)

<sup>1</sup>*Center for Underground Physics, Institute for Basic Science (IBS), Daejeon 34126, Korea*

<sup>2</sup>*Department of Physics, Sejong University, Seoul 05006, Korea*

<sup>3</sup>*Department of Physics and Astronomy, Seoul National University, Seoul 08826, Korea*

<sup>4</sup>*Department of Science Education, Ewha Womans University, Seoul 03760, Korea*

<sup>5</sup>*Department of Physics, Kyungpook National University, Daegu 41566, Korea*

<sup>6</sup>*Korea Research Institute of Standards and Science, Daejeon 34113, Korea*

<sup>7</sup>*University of Science and Technology (UST), Daejeon 34113, Korea*

<sup>8</sup>*Department of Accelerator Science, Korea University, Sejong 30019, Korea*

(Dated: May 8, 2019)

Limits on the cross section for weakly interacting massive particles (WIMPs) scattering off nucleons in the NaI(Tl) detectors at the Yangyang Underground Laboratory are obtained with a 2967.4 kg · day data exposure. Nuclei recoiling are identified by the pulse shapes produced by scintillation light signals. Data are consistent with no nuclear recoil hypothesis, and 90% confidence level upper limits are set. These limits partially exclude the DAMA/LIBRA allowed region for WIMP-sodium interactions with the same NaI(Tl) target material. The 90% confidence level upper limit on the WIMP-nucleon spin-independent cross section is  $3.26 \times 10^{-4}$  pb for a WIMP mass at 10 GeV/c<sup>2</sup>.

## I. INTRODUCTION

A number of astrophysical observations provide evidence that the dominant matter component of the universe is not ordinary matter, but rather non-baryonic dark matter [1, 2]. Theoretically favored dark matter candidates are weakly interacting massive particles (WIMPs) [3], which were well motivated by supersymmetric models [4]. Many direct searches for WIMP dark matter in deep underground laboratories have been performed and failed to confirm evidence for a signal [5], with the sole exception of DAMA (including DAMA/NaI and DAMA/LIBRA). This experiment has been operating over 20 years and has consistently reported a positive signal of annual modulation of WIMP [6–9] with a statistical significance that is more than  $9\sigma$  [9]; recently this significance has been strengthened with an additional six-year data exposure [10]. This signal can be interpreted as being due to WIMP-nucleon scattering in the context of the standard halo structure of the WIMP dark matter model [11]. However, the inferred WIMP-nucleon cross sections in this case are in conflict with other null observations using different target materials [12–15]. Considering the high significance of the signal as well as the impact of possible observation of WIMP dark matter, an independent verification of the DAMA signal using the same NaI(Tl) target material is required. A number of efforts with NaI target materials aimed at achieving this

goal are in progress [16–22].

Even in the event that ongoing efforts verify the annual modulation of event rates in the NaI(Tl) crystals, it will remain of particular interest to study the characteristics of the nuclear recoil (NR) events that produce this modulation. The recoil signals that the DAMA experiment sees could be due either to nuclear or electron recoils and, thus, allow for interpretations by models that attribute the modulation signals to WIMP-electron interactions [23, 24]. If the DAMA modulation signal is confirmed, experimental studies that can distinguish electron recoils from nuclear recoils will be necessary.

The Korea Invisible Mass Search (KIMS) collaboration has developed low-background NaI(Tl) crystals with the purpose of reproducing the DAMA’s modulation results [19, 25]. A good understanding of background contaminants of the crystals has been achieved [26]. The characteristics of NR signals are measured with a neutron source and found to have time-profile characteristics that are different than those from electron recoils (ER) produced by  $\gamma$ -rays from a <sup>137</sup>Cs source [27]. Similar time-profile differences in scintillating CsI(Tl) crystal signals have been used to discriminate between NR and ER events, so-called pulse shape discrimination (PSD), on a statistical basis as described in Ref. [12, 28], and set upper limits on WIMP-nucleon cross sections in the context of the standard halo model [29]. This paper presents a search for WIMP-nucleon interaction with two low-background NaI(Tl) crystals corresponding to 2967.4 kg · days exposure by using a direct extraction of the NR events with a PSD analysis.

\* kwkim@ibs.re.kr

† hyunsulee@ibs.re.kr

## II. EXPERIMENT

The two crystals are cylindrical in shape but different dimensions; one is 12.7 cm in diameter and 17.8 cm in length with a mass of 8.26 kg; the other is 10.7 cm in diameter and 27.9 cm in length with a mass of 9.15 kg, as described in Table I. The crystals are encapsulated within a cylindrical copper structure with a quartz window at each end. A 76 mm Hamamatsu R12669 photomultiplier tube (PMT) is mounted at each end of the cylinder. The assembled detector modules are installed in the shielding structure that was used for the KIMS CsI(Tl) detector measurements at the Yangyang Underground Laboratory [12, 30, 31]. This includes a 12-module array of low-background CsI(Tl) detectors inside a shield that consists, from inside out, of 10 cm of copper, 5 cm of polyethylene, 15 cm of lead, and 30 cm of mineral oil to stop external radiation. The data were collected between November 2013 and January 2015 with configurations described in Ref. [25].

TABLE I. The crystals used in this analysis and the amount of data for each crystal

Name	Size (D)×(L)	Mass (kg)	Light Yield (photoelectrons/keV)	Exposure (days)
NaI1	12.7 cm×17.8 cm	8.26	15.6±1.4	80.8
NaI2	10.7 cm×27.9 cm	9.15	15.5±1.4	251.4

Signals from each PMT are amplified by a custom-made preamplifier and digitized by a 400-MHz flash analog-to-digital converter. An event is triggered if a single photoelectron in each PMT is observed within a 200 ns time window. The energy scales for the crystals are determined using 59.5 keV  $\gamma$  events from a  $^{241}\text{Am}$  calibration source. The internal 68.7 keV line caused from cosmogenic  $^{125}\text{I}$  and the 46.5 keV line from  $^{210}\text{Pb}$  are used for time-dependent monitoring of the energy scale.

We obtained light yields of the crystals of about 15.5 photoelectrons/keV [25] that is approximately twice larger than that of crystals that were used in previous studies by NAIAD [32] and DAMA [33]. This high light yields allow us to discriminate the NR events with much better PSD capability [27]. The background levels of the crystals are approximately 10 and 8 counts/kg/day/keV at 2–4 keV energy region but decreased to 7 and 4 counts/kg/day/keV at 4–10 keV energy region for NaI1 and NaI2, respectively [25]. These background levels are lower than those of the crystals used by NAIAD experiment [32], but higher than DAMA/LIBRA [9]. Details of background studies for the crystals are reported elsewhere [22, 25, 26].

In order to have a good reference distribution of each known background and signal, we took calibration data of ER, NR, and surface  $\alpha$  decays (SR). ER events were obtained with the same crystals used in this analysis by

irradiating them with a  $^{137}\text{Cs}$  source in the copper chamber. Here the setup and running conditions were the same as those for the WIMP search a data.

NR events were obtained with a small piece of NaI(Tl) crystal ( $2\times 2\times 1.5\text{ cm}^3$ ), taken from the same ingot as NaI2, that was irradiated in a monoenergetic 2.43 MeV neutron beam. In order to identify neutrons scattered from NaI, we used neutron tagging detectors made of BC501A liquid scintillator. A time coincidence between the crystal to one of the neutron detectors was required to reject randomly selected events. Details of the neutron calibration with similar setup were reported previously [27, 34, 35].

It is known that  $\alpha$  decays of  $^{210}\text{Po}$  on the crystal surface can mimic WIMP events in the region of interest (ROI) [36–38]. To determine the pulse shape characteristics of SR events, we contaminated a NaI(Tl) crystal with  $^{222}\text{Rn}$  and waited for two weeks until  $^{210}\text{Po}$   $\alpha$  decays were the dominant activity. We then studied its response for events tagged as outgoing  $^{210}\text{Po}$   $\alpha$  recoils from the crystal surface and obtained a sample distribution of SR induced signals [39].

## III. ANALYSIS

In order to discriminate PMT-induced noise from radiation induced signal events, event selection criteria using the separation parameters described in Ref. [25] are applied. The most important parameters are the difference between the “slow” (100–600 ns) charge sum and “fast” (0–50 ns) charge sum and the charge asymmetry between the two PMTs. A NR event from the WIMP interaction is expected to produce a hit in a single crystal, designated as a single-hit (SH) event. Events with accompanying hits in other surrounding NaI(Tl) or CsI(Tl) crystals are designated as multiple-hit (MH) events. The MH events are used to determine the selection efficiency and for modeling ER events. The efficiency determined with the MH events is greater than 90% in the signal ROI (2–8 keV). The NR events from the neutron beam are used for an independent determination of the efficiency for NR events and show consistent results with the determination for ER events within 2%.

We use the PSD method to determine the contributions of WIMP-induced NR events. To characterize the PSD performance, we first define a photon cluster as an isolated pulse typically equivalent to a single photoelectron at the low-energy region [30]. Then, we use the natural logarithm of the mean time (LMT) of an event waveform calculated over 1  $\mu\text{s}$ , defined as

$$\log(\text{Mean Time}) = \text{LMT} = \log\left(\frac{\sum_{i=1}^n A_i t_i}{\sum_{i=1}^n A_i} - t_1\right), \quad (1)$$

where  $A_i$  is the charge of the  $i$ th cluster and  $t_i$  is the time of the  $i$ th cluster.

Because we use different crystals for the NR and SR distributions with different environmental conditions,

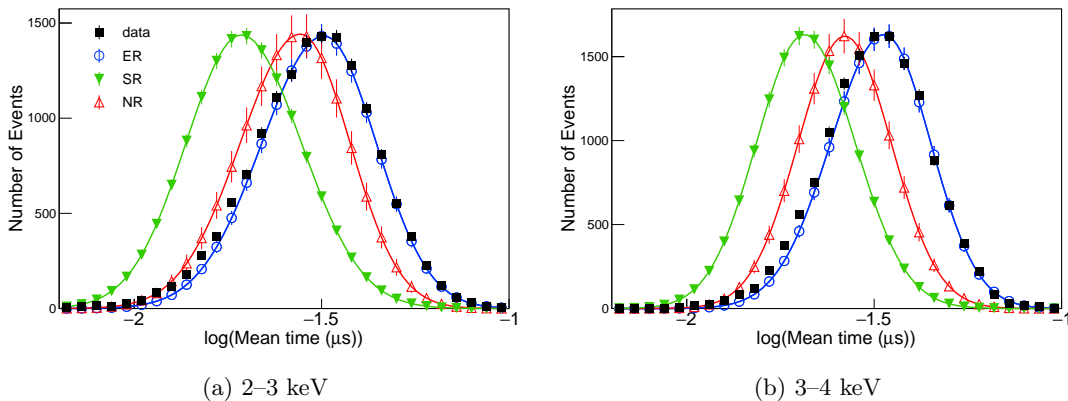


FIG. 1. The logarithm of mean time distributions of different recoil types and data are presented separately for 2–3 keV (a) and 3–4 keV (b) in NaI2. The ER (blue open circle), SR (green filled triangle), and NR (red open triangle) were modeled with asymmetric Gaussian functions and compared with the data (black filled square).

correction factors are applied for the NR and the SR events on the basis of differences in the ER spectra across different crystal measurements, assuming that the ratio  $R_\tau = \tau_n/\tau_e$  is independent of temperature [12, 40, 41], where  $\tau_n$  and  $\tau_e$  are decay times of the NR and ER, respectively. Figure 1 shows a comparison of the LMT distributions for different recoil-type events, together with data in energies of 2–3 keV and 3–4 keV for NaI2. Models for the recoil events are built using an asymmetric Gaussian function for every 1 keV energy bin.

Several sources of systematic uncertainties are considered for the PSD analysis. The dominant components are associated with mean and root mean square (RMS) uncertainties from the fitting for the LMT modeling because of the limited statistics of the calibration data. The NR distributions shifted by these uncertainties are shown in Fig. 2. We consider shape uncertainties for each of the three recoil-type events and each energy bin independently and incorporated these uncertainties into the analysis fitter as a systematic variation. The uncertainty caused by corrections due to slightly different distributions of the ER events for different recoil-type measurements are also considered. Uncertainties in the efficiency estimation and differences in the independent cross-check for different recoil-type samples are considered as possible rate changes. Variations in the energy calibrations and resolutions are also included as systematic errors.

To search for WIMP-induced NR events in the data, binned maximum-likelihood fits to the measured LMT spectra between 2 and 8 keV are performed. The Bayesian Analysis Toolkit [42] is used with probability density functions (PDFs) based on the LMT models for the NR, SR, and ER events shown in Fig. 1. The likelihood is built for each 1 keV bin for 2–8 keV of each crystal and multiplied as a single likelihood. Uniform priors are used for three different recoil types. The numbers of NR events across different energy bins and crystals are constrained by using the shapes of simulated WIMP en-

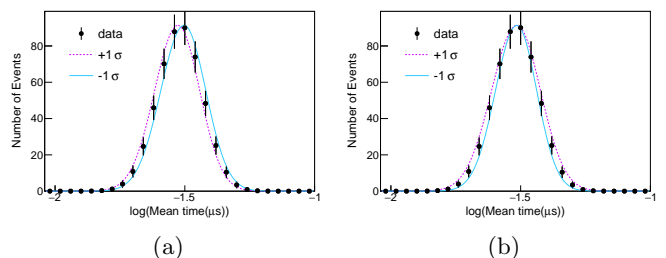


FIG. 2. The distributions shifted by the mean (a) and RMS (b) uncertainties for NR events in the 7 to 8 keV energy region, where the largest shape changes occur.

ergy spectra. The measured energy spectrum of the SR from Ref. [39] is used to constrain the energy-dependent rate of the SR events in each crystal. However, the total amount of SR events for each crystal is freely floated.

We obtain the expected energy spectrum for WIMP interactions by generating samples for 17 different WIMP masses, ranging from 5 GeV/ $c^2$  to 1,000 GeV/ $c^2$  using the same parameters that are used for the WIMP interpretation of the DAMA signals [11] in the framework of the standard halo model [29]. The systematic uncertainties are included in the fit as nuisance parameters with Gaussian priors assumed for both the rate and the shape changes. We consider the possibility of correlated rate and shape uncertainties as well as uncorrelated bin-by-bin statistical uncertainties.

#### IV. RESULTS

Data fits are performed for each assumed WIMP mass value. Figure 3 (a) shows the posterior PDF of the NR rate in the case for a WIMP mass of 10 GeV/ $c^2$  as an example. The maximum value of the posterior PDF for

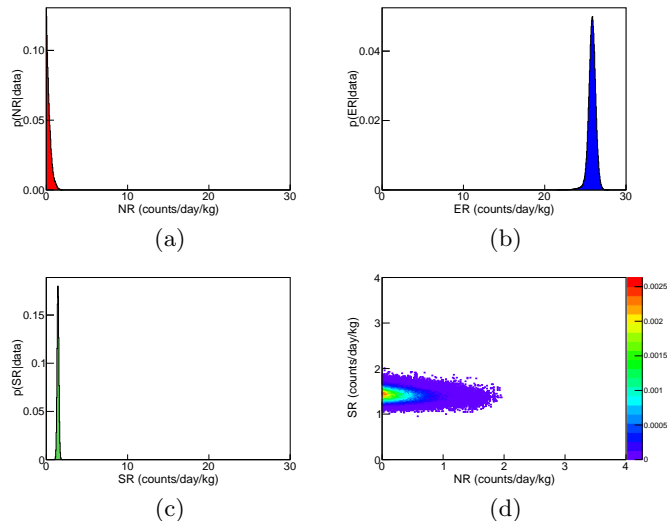


FIG. 3. The posterior PDFs for: (a) NR events; (b) ER events; and (c) SR events for 2–8 keV of NaI2 normalized to time (day) and mass (kg). (d) Two-dimensional distribution of posterior NR and SR PDFs, where no correlation is evident.

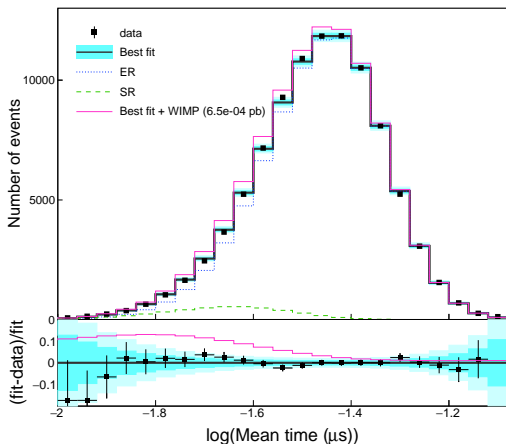


FIG. 4. The accumulated LMT spectrum for all energy bins in the ROI and the two crystals from the data (square point) and best fit model (solid line with shaded band corresponding to 1- and 2- $\sigma$  uncertainties). The fitted results for ER events (blue dotted line) and SR events (green dashed line) are indicated. The magenta thin solid line represents the expected signal excess above background for a 10 GeV/ $c^2$  WIMP mass and  $6.5 \times 10^{-4}$  pb cross section which corresponds to two times of 90% limit value. The lower panel shows the residuals between the data and the background model.

the NR component is zero. Figures 3 (b) and (c) show those for the ER and SR backgrounds, which both have non-zero contributions. The two-dimensional posterior PDFs for NR and SR are given in Fig. 3 (d), where no evident correlation has been found. The result of the

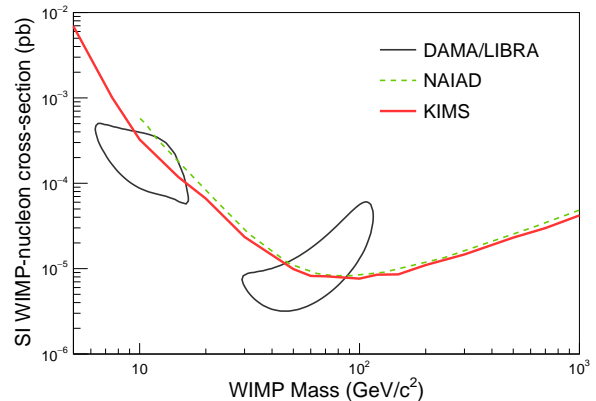


FIG. 5. Observed (red solid line) 90% CL exclusion limits on the WIMP-nucleon spin-independent cross sections. The contour from WIMP-induced DAMA  $3\sigma$  allowed signal region [11] and the limit from the previous NaI(Tl) detector from the NAIAD experiment [32] are shown.

maximum likelihood fit of the LMT spectrum for the 10 GeV/ $c^2$  WIMP mass case is shown in Fig. 4. Here, the summed spectrum for the two crystals over the 2–8 keV ROI are shown together with the best-fit, non-NR signal result. For comparison, the expected signal for a 10 GeV/ $c^2$  WIMP mass and a spin-independent cross section of  $6.5 \times 10^{-4}$  pb which corresponds to two times of 90% limit value added to the best fit is overlaid.

For all 17 WIMP mass values that are considered, the likelihood fits found no excess corresponding to NR signal events; all the posterior PDFs for the NR rates are consistent with zero. We determine 90% CL upper limits on spin-independent WIMP-nucleon cross sections, such that 90% of the posterior densities fall below the limit, as shown in Fig. 5. The obtained limits are compared with the  $3\sigma$  contours of the allowed regions associated with the DAMA signal and the limits from the NAIAD experiment [32] that used the NaI(Tl) crystals with 16388.5 kg·days exposure using the PSD analysis. Even though data exposure is only 20% of the NAIAD experiment, we obtain overall slightly better limits by taking advantage of lower background and higher light yields that provided better PSD of NR events [27].

## V. CONCLUSION

We report limits on WIMP-nucleon cross sections using a data sample collected with two low-background NaI(Tl) crystals with a total exposure of 2967.4 kg·days. No excess of the NR events is observed, and 90% CL upper limits on the WIMP-nucleon cross section are set. The limit,  $3.26 \times 10^{-4}$  pb for a WIMP mass at 10 GeV/ $c^2$ , partially covers the DAMA  $3\sigma$  region of WIMP-sodium interaction and demonstrates the feasibility of using PSD tech-

niques for the direct extraction of WIMP-nucleon scattering from ongoing NaI(Tl) experiments such as COSINE-100 [22] and ANAIS-112 [43].

oratory space at Yangyang. This research was supported by the Institute for Basic Science (Korea) under project code IBS-R016-A1.

## ACKNOWLEDGMENTS

We thank the Korea Hydro and Nuclear Power (KHNP) Company for providing the underground lab-

- 
- [1] D. Clowe *et al.*, *Astrophys. J.* **648**, L109 (2006).
- [2] P. A. R. Ade *et al.* (Planck Collaboration), *Astron. Astrophys.* **594**, A13 (2016).
- [3] B. W. Lee and S. Weinberg, *Phys. Rev. Lett.* **39**, 165 (1977).
- [4] G. Jungman, M. Kamionkowski, and K. Griest, *Phys. Rept.* **267**, 195 (1996).
- [5] G. Bertone, D. Hooper, and J. Silk, *Phys. Rep.* **405**, 279 (2005).
- [6] R. Bernabei *et al.* (DAMA Collaboration), *Phys. Lett. B* **480**, 23 (2000).
- [7] R. Bernabei *et al.* (DAMA/LIBRA Collaboration), *Eur. Phys. J. C* **56**, 133 (2008).
- [8] R. Bernabei *et al.* (DAMA/LIBRA Collaboration), *Eur. Phys. J. C* **67**, 39 (2010).
- [9] R. Bernabei *et al.* (DAMA/LIBRA Collaboration), *Eur. Phys. J. C* **73**, 2648 (2013).
- [10] R. Bernabei *et al.* (DAMA/LIBRA Collaboration), (2018), arXiv:1805.10486 [hep-ex].
- [11] C. Savage, G. Gelmini, P. Gondolo, and K. Freese, *JCAP* **0904**, 010 (2009).
- [12] S. C. Kim *et al.* (KIMS Collaboration), *Phys. Rev. Lett.* **108**, 181301 (2012).
- [13] D. S. Akerib *et al.* (LUX Collaboration), *Phys. Rev. Lett.* **118**, 021303 (2017).
- [14] A. Tan *et al.* (PandaX Collaboration), *Phys. Rev. Lett.* **117**, 121303 (2016).
- [15] E. Aprile *et al.* (XENON Collaboration), *Phys. Rev. Lett.* **119**, 181301 (2017).
- [16] E. Barbosa de Souza *et al.* (DM-Ice Collaboration), *Phys. Rev. D* **95**, 032006 (2017).
- [17] J. Amare *et al.* (ANAIS Collaboration), *Nucl. Instrum. Meth.* **A742**, 187 (2014).
- [18] J. Xu, F. Calaprice, F. Froberg, E. Shields, and B. Suerfu (SABRE Collaboration), *Proceedings, 5th Topical Workshop on Low Radioactivity Techniques (LRT 2015): Seattle, WA, USA, March 18-20, 2015*, AIP Conf. Proc. **1672**, 040001 (2015).
- [19] P. Adhikari *et al.* (KIMS Collaboration), *Eur. Phys. J. C* **76**, 185 (2016).
- [20] K. Fushimi *et al.* (PICO-LON Collaboration), *J. Phys. Conf. Ser.* **718**, 042022 (2016).
- [21] G. Angloher *et al.* (COSINUS Collaboration), *JINST* **12**, P11007 (2017).
- [22] G. Adhikari *et al.* (COSINE-100 Collaboration), *Eur. Phys. J. C* **78**, 107 (2018).
- [23] N. F. Bell, Y. Cai, R. K. Leane, and A. D. Medina, *Phys. Rev. D* **90**, 035027 (2014).
- [24] B. M. Roberts, V. A. Dzuba, V. V. Flambaum, M. Pospelov, and Y. V. Stadnik, *Phys. Rev. D* **93**, 115037 (2016).
- [25] K. W. Kim *et al.* (KIMS Collaboration), *Astropart. Phys.* **62**, 249 (2015).
- [26] G. Adhikari *et al.* (KIMS Collaboration), *Eur. Phys. J. C* **77**, 437 (2017).
- [27] H. S. Lee *et al.* (KIMS Collaboration), *JHEP* **08**, 093 (2015).
- [28] H. S. Lee *et al.* (KIMS Collaboration), *Phys. Rev. Lett.* **99**, 091301 (2007).
- [29] J. Lewin and P. Smith, *Astropart. Phys.* **6**, 87 (1996).
- [30] H. S. Lee *et al.* (KIMS Collaboration), *Phys. Lett. B* **633**, 201 (2006).
- [31] H. S. Lee *et al.* (KIMS Collaboration), *Nucl. Instrum. Meth. A* **571**, 644 (2007).
- [32] G. J. Alner *et al.* (UK Dark Matter Collaboration), *Phys. Lett. B* **616**, 17 (2005).
- [33] R. Bernabei *et al.* (DAMA Collaboration), *Phys. Lett.* **B389**, 757 (1996).
- [34] J. H. Lee *et al.*, *Nucl. Instrum. Meth.* **A782**, 11 (2015).
- [35] H. S. Lee *et al.* (KIMS Collaboration), *JINST* **9**, P11015 (2014).
- [36] V. A. Kudryavtsev *et al.* (UK Dark Matter Collaboration), *Astropart. Phys.* **17**, 401 (2002).
- [37] S. C. Kim *et al.* (KIMS Collaboration), *Astropart. Phys.* **35**, 781 (2012).
- [38] R. Strauss *et al.* (CRESST Collaboration), *Eur. Phys. J. C* **75**, 352 (2015).
- [39] K. W. Kim, C. Ha, N. Y. Kim, Y. D. Kim, H. S. Lee, B. J. Park, and H. K. Park (KIMS Collaboration), *Astropart. Phys.* **102**, 51 (2018).
- [40] B. Ahmed *et al.* (UK Dark Matter Collaboration), *Astropart. Phys.* **19**, 691 (2003).
- [41] H. S. Lee, *Dark Matter Search with CsI(Tl) Crystals*, Ph.D. thesis, Seoul Natl. U. (2007).
- [42] A. Caldwell, D. Kollar, and K. Kroninger, *Comput. Phys. Commun.* **180**, 2197 (2009).
- [43] I. Coarasa *et al.* (ANAIS Collaboration), (2017), arXiv:1704.06861 [astro-ph.IM].